Research Article

CARNIAN EVENTS

Jacopo Dal Corso

State Key Laboratory of Geomicrobiology and Environmental Changes, China University of Geosciences, Wuhan, China; j.dalcorso@cug.edu.cn

Abstract – The Carnian Pluvial Episode (CPE; Late Triassic) was an interval of C-cycle perturbations, global warming and biological turnover, occurring between ca. 234 and 232 Ma. The C-cycle perturbations are recorded as discrete sharp negative C-isotope excursions (NCIEs) in marine and terrestrial sedimentary successions around the world, and at least two warming phases are shown by O-isotope data from conodont apatite. The estimated duration of each CPE's NCIE is similar to the duration of NCIEs associated with other Mesozoic major environmental and biological changes. Also similar with other events are the calculated rates of CO_2 emissions into the atmosphere–ocean system during each NCIE. The successive C-cycle perturbations could have had different impacts on environments and ecosystems. Hence, considering the CPE as a single "event" results in flawed understanding of the triggers and mechanisms of Carnian paleoenvironmental changes, and bias comparative studies. I here argue that a change in perspective is necessary, including considering the Carnian C-cycle perturbations as separate events, and revising the current most common subdivision of the Carnian stage into new substages that allow for better stratigraphic control. This is relevant because the events that occurred during the Carnian might have caused the rise of flora and fauna that later dominated terrestrial and marine ecosystems, e.g., dinosaurs and pelagic calcifiers. The fact that these events occurred within a maximum timeframe of 2.5 million years remains significant, and their temporal closeness should be acknowledged

INTRODUCTION

Environmental perturbations, extinctions and radiations occurred in the Carnian, ca. 237–227 Ma (Simms & Ruffell, 1989; Dal Corso et al., 2020). The interval of major climate change and biological turnovers is named the Carnian Pluvial Episode (CPE)—but also other names have been used in the literature, e.g., Reingraben Turnover or Event, Carnian crisis, Carnian Humid Event, Mid-Carnian Event, and Carnian Wet Intermezzo (Schlager & Schöllnberger, 1974; Simms & Ruffell, 1989; Hornung & Brandner, 2005; Hornung et al., 2007a,b; Kozur & Bachmann, 2010; Ogg, 2015; Ruffell et al., 2016; Sun et al., 2016; Dal Corso et al., 2018a, 2020)—and occurred between ca. 234 and 232 Ma (Figure 1). The CPE was first defined as an episode of more humid (pluvial) conditions within the generally arid climate of the Late Triassic, coeval with extinctions among marine and terrestrial animals (Simms & Ruffell, 1989). The original hypothesis of a widespread CPE made by Simms and Ruffell initially nearly fell into obscurity (Simms & Ruffell, 2018), but evidence of a Carnian global perturbation of the climate has steadily grown since then.

A major step-forward in the definition and understanding of the CPE has been through stable C-isotope ($\delta^{13}C$) stratigraphy. The $\delta^{13}C$ signature of marine carbonates, and marine and terrestrial organic matter from different Carnian successions around the world show clear and consistent shifts. Multiple sharp negative C-isotope excursions (NCIEs), starting across the Julian 1–Julian 2 boundary (i.e., boundary between the Thetyan *Trachyceras aonoides*–*Austrotrachyceras austriacum* ammonoid Zones) of the early Carnian and terminating at the base of the Tuvalian 2 (*Tropites subbullatus* Zone) of the late Carnian, are found in the sedimentary record (Figure 1; Dal Corso et al.,

Published online: 5 May, 2025

Dal Corso, J. 2025. Carnian Events. *Albertiana*, vol. 49, 1–11.

2012, 2015, 2018b, 2020; Mueller et al., 2016b, 2016a; Sun et al., 2016, 2019; Miller et al., 2017; Baranyi et al., 2019; Shi et al., 2019; Fu et al., 2020; Jin et al., 2020, 2022, 2023; Lu et al., 2021; Tomimatsu et al., 2021; Lestari et al., 2024; Rahman et al., 2024; Zhang et al., 2024). 4 NCIEs are recorded during the CPE interval in most of sections with good age control and correlatability (e.g., Sun et al., 2016; Dal Corso et al., 2018b). In some records a (smaller) 5th NCIE has been suggested, and further late Tuvalian NCIEs are recorded, needing confirmation and better age (Baranyi et al., 2019; Hounslow et al., 2022; Hounslow and Gallois, 2023; Zhang et al., 2024). The magnitude of the negative $\delta^{13}C$ shifts varies between NCIEs and localities, but it is in general >2‰ (Figure 1). The global occurrence of synchronous NCIEs, and the fact that they are recorded in different archives (carbonates and organic matter) and geological settings (marine and terrestrial), indicate discrete substantial injections of ^{13}C-depleted carbon into the reservoirs of the exogenic C-cycle (Dal Corso et al., 2012, 2022). The discovery of the Carnian NCIEs has allowed a better understanding of the nature of the CPE, but also provided a chemostratigraphic tool to identify its boundaries and correlate sections. Previous definitions of the CPE interval were based mainly on sedimentological and palynological changes that were, by their own nature, strongly influenced by local environmental and depositional conditions.

The NCIEs occurred in a relatively long interval of up to 2.5 Myr (likely 1.2–1.6 Myr according to recent stratigraphies; Miller et al., 2017; Bernardi et al., 2018; Hounslow and Gallois, 2023; Dal Corso et al., 2024; Zhang et al., 2024). Each NCIE seems linked to discrete environmental changes as evidenced by, for example, distinct siliciclastic inputs in marine basins, marine extinctions, pulses of higher nutrient fluxes to lacustrine environments and multiple shifts in sporomorphs assemblages from xerophytic to hygrophytic (Roghi et al., 2010; Dal Corso et al., 2018b, 2020; Baranyi et al., 2019; Lu et al., 2021).

A number of increasingly higher resolution studies indicate that the vision of the CPE as a single "pluvial" episode is incorrect. Here, I argue that current knowledge requires a necessary change in perspective on the CPE: as a time interval punctuated by discrete events that could have had different unrelated triggers, and which each could had different effects on the environments and biota. Indeed, each discrete event within the CPE is comparable, in duration and genesis, to other major C-isotope perturbations of the Phanerozoic.

MULTIPLE C-CYCLE PERTURBATIONS DURING THE CARNIAN

The NCIEs of the CPE indicate injections of isotopically light carbon into the reservoirs of the exogenic carbon cycle, but pinpointing the source of the ^{13}C-depleted carbon is difficult. Age overlap between the CPE and the emplacement of Wrangellia large igneous province (Furin et al., 2006), an oceanic plateau that erupted at equatorial latitudes in the Panthalassa (Lassiter et al., 1995; Greene et al., 2010; Tomimatsu et al., 2021), points to a volcanic source of CO_2 (Dal Corso et al., 2012, 2020; Lu et al., 2021; Mazaheri-Johari et al., 2021; Jin et al., 2023). The C-isotope signature of Wrangellia's CO_2 is unknown, but mantle carbon appears to be on average more ^{13}C-enriched than the depleted source that it is required to generate the NCIEs. The minimum likely volume of basalt erupted by Wrangellia (Lassiter et al., 1995) would have degassed about 5000 Gt C (Dal Corso et al., 2012). Considering such an amount of volcanic CO_2 (split into four pulses of 1250 GtC each on the assumption of 4 discrete NCIEs) with $\delta^{13}C$ set at -5‰, box modelling can reproduce 4 NCIEs, but with magnitudes of ≤1‰ (Dal Corso et al., 2022), so smaller than those actually recorded (>2‰; Figure 1). Mass balance calculations indicate that C emissions of about 3500–17500 Gt C would be needed to produce CPE's negative C-isotope shifts, depending on the C-isotope signature of the source (Miller et al., 2017).

Positive feedback with destabilization of ocean floor methane hydrates and consequent release of extremely ^{13}C-depleted carbon (Dickens et al., 1995) cannot be excluded for the CPE (Dal Corso et al., 2012), but it is also difficult to prove as the process does not leave an independent signature in the sedimentary record. Current understanding of Wrangellia emplacement (Greene et al., 2010) does not suggest significant production of thermogenic CO_2 from the interaction of the rising magma and surrounding sediments, as observed for other LIPs, e.g., Siberian Traps (e.g., Burgess et al., 2017; Svensen et al., 2018) and Central Atlantic Magmatic Province (e.g., Davies et al., 2017; Heimdal et al., 2020).

In marine sedimentary successions that are well-constrained with ammonoid and conodont biostratigraphy, the first NCIE of the CPE is found across the Julian 1–2 boundary (i.e., boundary between the *Trachyceras aonoides* and *Austrotrachyceras austriacum* ammonoid Zones), the second NCIE within the Julian 2 (i.e., *Austrotrachyceras austriacum* ammonoid Zone), the third NCIE across the Julian 2–Tuvalian 1 boundary (i.e., boundary between the *Austrotrachyceras austriacum* and *Tropites dilleri* ammonoid Zones) and the fourth NCIE at the base of the Tuvalian 2 (i.e., *Tropites subbullatus* ammonoid Zone; Figure 1). In the GTS2020, Geologic Time Scale (Ogg et al., 2020), the estimated lengths of the Carnian biochronozones are: Julian 1 = 2.8 Myr, Julian 2 = 0.6 Myr, Tuvalian 1 = 0.8 Myr. Magnetostratigraphic study of successions in the Germanic Basin gives a longer duration for the Tuvalian 1 of 1.9 Myr (Zhang et al., 2020). Other integrated stratigraphy (Bernardi et al., 2018) gives durations of 3 Myr for the Julian 1, 0.9 Myr for the Julian 2, and 1 Myr for the Tuvalian 1. These three proposed timescales show a relatively long Julian 2 – Tuvalian 1 (i.e. CPE) interval of 1.4–2.5 Myr (see also discussion in Dal Corso et al., 2024). New magnetostratigraphic analysis from the Dolomites allowed updating the Geomagnetic Polarity Timescale, giving a new age for the Ladinian–Carnian boundary of ca. 236.5 Ma (Maron et al., 2024), thus shortening by ca. 0.5 Myr the above-mentioned previous estimates for the duration of the Julian 1.

Cyclostratigraphy from a terrestrial succession in England (UK) gives durations of about 0.4 Myr for both the Julian 2 and the Tuvalian 1 (Miller et al., 2017), with a total duration of the CPE of about 1.1 Myr. Additionally, this cyclostratigraphy shows that each NCIE recorded in this section (a total of 4) had durations of 41–130 Kyr (Miller et al., 2017). These estimates are

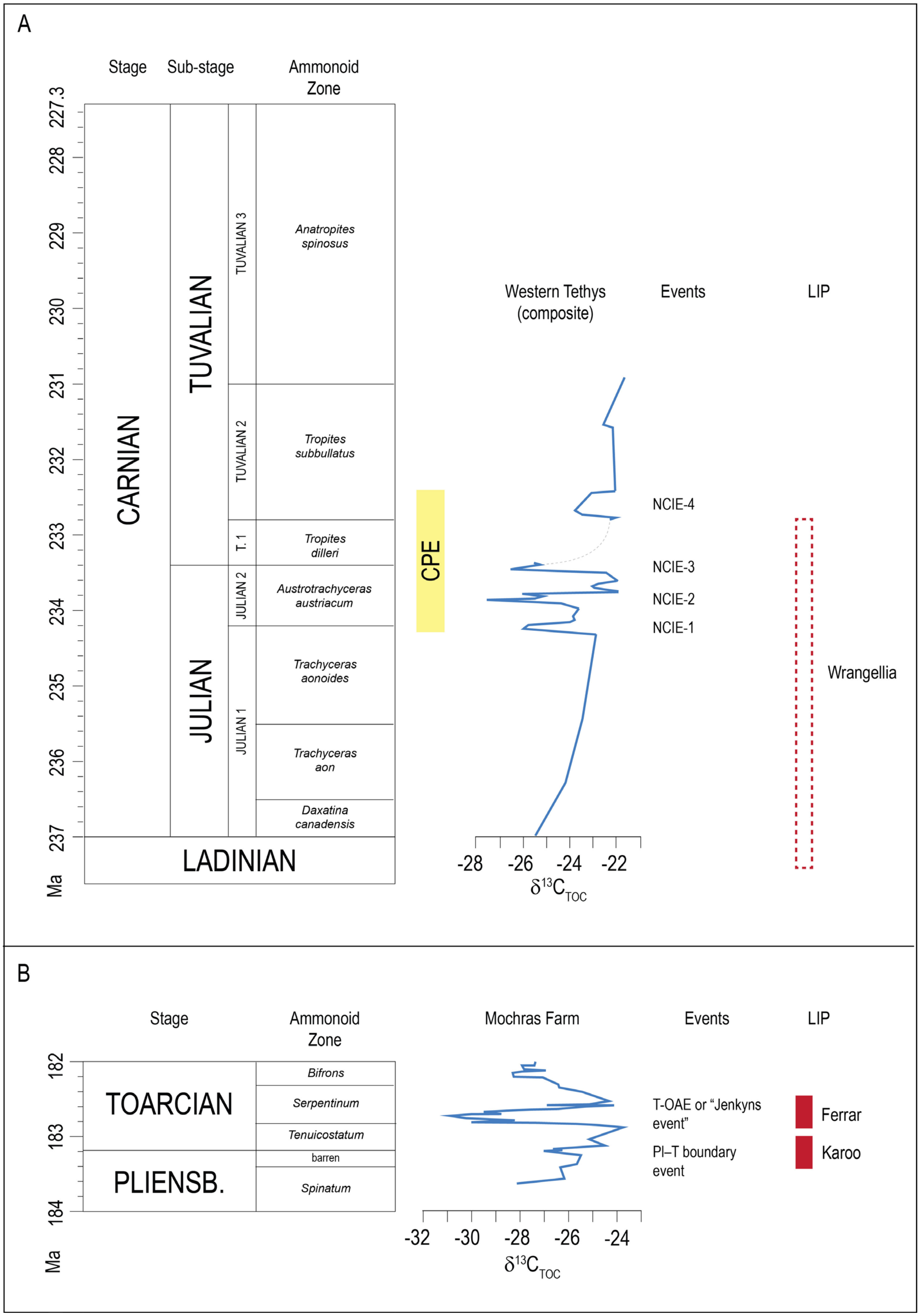

Figure 1– A) Carnian timescale—substages and Tethyan ammonoid Zones after the Geologic Time Scale 2020 (Ogg et al., 2020)—age of the Carnian Pluvial Episode (CPE), reference C-isotope curve across the CPE from the Western Tethys showing the negative C-isotope excursions (NCIE 1–4) that mark the interval (Dal Corso et al., 2018b), and maximum age span of Wrangellia LIP (Greene et al., 2010; Dal Corso et al., 2020). Note that recently updated Geomagnetic Polarity Timescale estimates the age of the Ladinian–Carnian boundary at ca. 236.5 Ma (Maron et al., 2024). T. = Tuvalian. B) NCIEs and LIP volcanism during the Pliensbachian – Toarcian of the Jurassic (Kemp et al., 2024b).

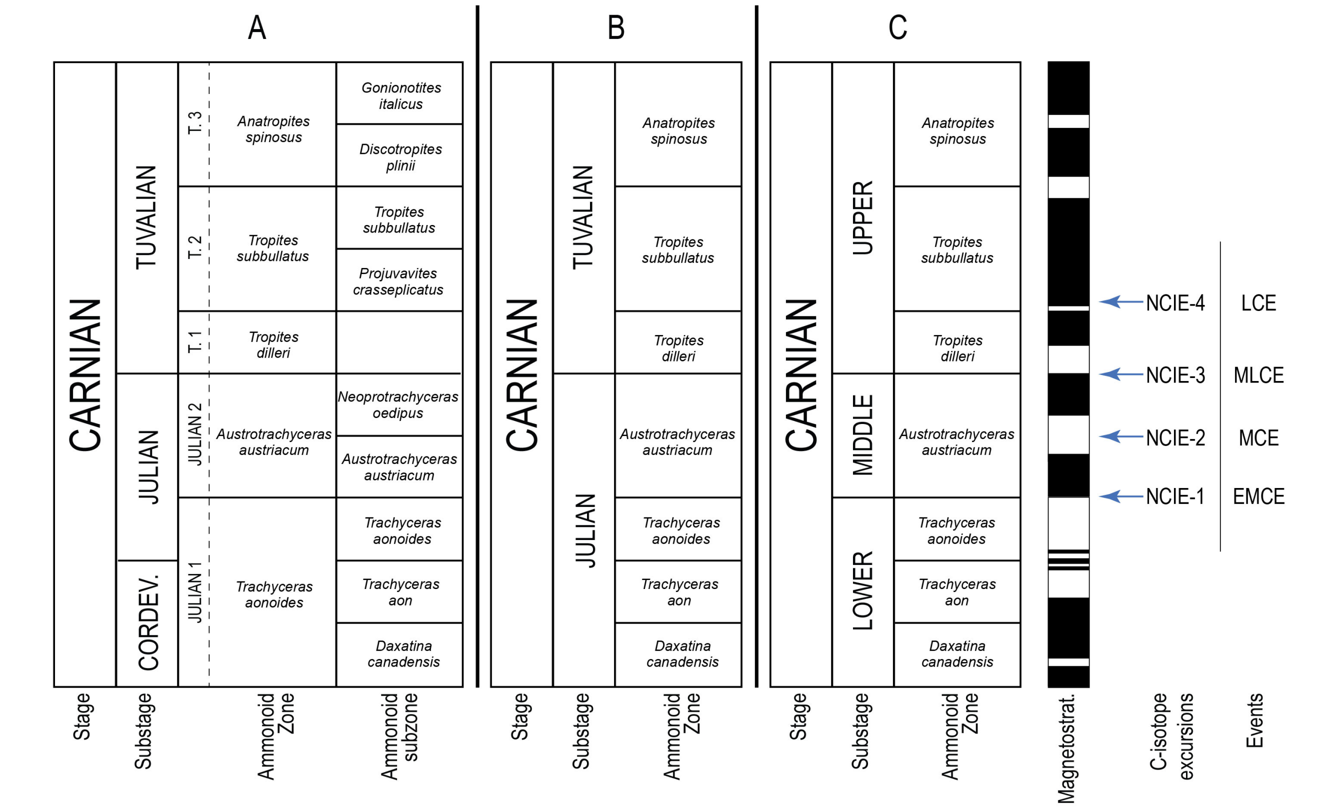

Figure 2 – Different Carnian subdivisions at substage level. A) Subdivision with ammonoid Zones after Gallet et al. (1994; see also, e.g., Hornung & Brandner, 2005), with Julian 1–2 and Tuvalian 1–3, and *Daxatina canadensis* as the first ammonoid subzone of the *Trachyceras aonoides* Zone (sensu Mietto et al., 2012), including the original substage subdivision of Mojsisivics et al. (1895) with the Cordevolian (e.g., Hornung et al., 2007b). B) Subdivision shown in the Geologic Timescale (GTS) 2020 (Ogg et al., 2020). C) Proposed subdivision into "Lower", "Middle", and "Upper" Carnian substages. T. = Tuvalian. Magnetostratigraphy is from Zhang et al. (2015, 2020). Age of the negative C-isotope excursions (NCIEs) as in Figure 1. EMCE = Early–Middle Carnian Event, MCE = Middle Carnian Event, MLCE = Middle–Late Carnian Event, LCE = Late Carnian Event.

shorter than those obtained by cyclostratigraphy in the Carnian marine succession of the Tibetan Plateau, with durations for each CIEs of 87–318 Kyr, and a total duration of the CPE of ca. 1.2 Myr (Zhang et al., 2024).

Each NCIE was separated by relatively long intervals of rather stable $\delta^{13}C$ of ca. 100–800 Kyrs (Figure 1; Miller et al., 2017; Bernardi et al., 2018; Dal Corso et al., 2024; Zhang et al., 2024). The CPE is therefore a long interval punctuated by relatively short NCIEs (Figure 1).

COMPARISON WITH OTHER EVENTS

Miller et al. (2017) first pointed out that the inferred duration of each NCIE of the CPE is similar to the duration of NCIEs that mark major ancient hyperthermals, such as the Palaeocene–Eocene Thermal Maximum (PETM, ca. 200 kyr; e.g., Li et al., 2022), the Toarcian oceanic anoxic event (T-OAE, or Jenkyns Event, 288±119 Kyr; e.g., Kemp et al., 2024b), the end-Triassic mass extinction (ETME, ca. 20–100 Kyr; Ruhl et al., 2010; Yager et al., 2017) and the Permian–Triassic boundary mass extinction (PETM, ca. 80 Kyr; Burgess et al., 2014). Moreover, some of these prominent Phanerozoic NCIEs occurred close in time to other NCIEs, and these temporally close NCIEs produced distinct environmental-biological changes and are often considered genetically different.

I here provide an example (Figure 1). The duration of the CIE that marks the T-OAE—an event that had many similarities with the CPE (e.g., comparable extinction rates among marine ecosystems and similar vegetation responses, enhanced hydrological cycling, and both linked to the emplacement of LIPs; see, e.g., Dal Corso et al., 2020; Baranyi et al., 2024; Kemp et al., 2024a)—was 288±119 Kyr (Figure 1; Kemp et al., 2024b). Notably, the T-OAE CIE post-dated by ca. 200–250 Kyr an earlier CIE that occurred across the Pliensbachian–Toarcian (Pl–T) boundary, and which had a duration <200 Kyr (Martinez et al., 2017; Al-Suwaidi et al., 2022; Kemp et al., 2024b). The Pl–T and T-OAE CIEs were coeval with two LIPs, the Karoo and Ferrar, respectively (Kemp et al., 2024b).

The rates at which ^{13}C-depleted CO_2 was emitted into the exogenic reservoirs of the C-cycle during different Phanerozoic NCIEs may have differed considerably, as can be inferred from first principles given the widely differing NCIE magnitudes at different events. Considering only the NCIE-1 event of the CPE (Figure 1), with a duration of the negative $\delta^{13}C$ shift of 20.5–43.4 Kyr and estimated release of CO_2 of about 1250–17000 Gt C (see discussion above), the ^{13}C-depletd CO_2 would have been injected into the atmosphere–ocean system at a rate of about 0.06–0.8 Gt

C/year (shorter scenario) to 0.02–0.4 Gt C/year (longer scenario). These rates of C emission are comparable to those estimated for the C-cycle perturbations at the T-OAE (0.04–0.27 Gt C/year on average; ca. 6000–40000 Gt C over 150–200 Kyr) and the ETME (0.08–0.65 Gt C/year on average; ca. 2000–14000 Gt C over 10–110 Kyr; Hu et al., 2024).

Such CO_2 emissions into the Carnian atmosphere could increase global mean surface temperature by up to 5 °C during each NCIE, as indicated by box modelling (Dal Corso et al., 2022). Temperature records for the CPE are based on $\delta^{18}O$ of conodont apatite and are of low resolution, but they do show at least two distinct warming events of 4 °C and 7 °C (Hornung et al., 2007a; Sun et al., 2016). Higher resolution reconstructions of palaeotemperatures are needed. Similarly, higher-resolution studies across each NCIE are required to better understand the specific environmental and biological responses to the CO_2 emissions. Distinct humid pulses, for example, are observed in coincidence with each NCIE in the Western Tethys (Roghi et al., 2010; Dal Corso et al., 2018b), but the patterns of the climate change and consequent biological turnovers are only coarsely defined (Dal Corso et al., 2020). Marine animals seem to have experienced a first crisis during NCIE-1, but a more severe turnover at the Julian–Tuvalian boundary, in correspondence to NCIE-3, i.e. ca. 0.8 Myr after the onset of the CPE (Figure 1; Rigo et al., 2007, 2018; Balini et al., 2010; Jenks et al., 2015; Chen et al., 2016; Sun et al., 2016; Dal Corso et al., 2020; Tóth et al., 2024). A crisis in marine carbonate producers is recorded at NCIE-1, recovering within the CPE around NCIE-3 (Dal Corso et al., 2015; Gattolin et al., 2015; Jin et al., 2022).

CPE's $\delta^{13}C$ negative shifts were separated by ca. 100–800 Kyrs, including positive $\delta^{13}C$ rebounds and following stable intervals (Miller et al., 2017; Dal Corso et al., 2024; Zhang et al., 2024; Figure 1). The time that passed between the successive emissions of CO_2 into the Carnian atmosphere could have been sufficient for environments and biota to recover, at least partially, from the stress caused by global warming. For example, highly diverse and complex marine ecosystems were already established ca. 1 Myr after the PTME (Dai et al., 2023). Biotic recovery after the ETME could have taken 0.22–0.7 Myr (Atkinson and Wignall, 2019). An ecosystem with high productivity thrived in the Chicxulub crater 30 Kyr after the asteroid impact (ca. 66 Ma), i.e. after the Cretaceous–Palaeogene mass extinction (Lowery et al., 2018). It has been hypothesized that the extinctions during the CPE could have paved the way for the radiation of groups of animals and plants that today form modern-type ecosystems (Dal Corso et al., 2020), hence understanding the mechanisms and patterns of the Carnian diversification is of primary importance.

CARNIAN EVENTS AND STRATIGRAPHIC FRAMEWORK

Given the durations of the CIEs and inter-CIEs intervals and comparison with other similar Phanerozoic events, the C-cycle perturbations that mark the CPE must be considered as separate events to more accurately reconstruct and better understand the mechanisms of Carnian environmental and biological changes, and properly compare these Carnian events to others of the Phanerozoic. This new approach would highly benefit from a more refined and formal chronostratigraphy. Given the large amount of data that has been collected in the last years, considering the CPE as a single phenomenon obfuscates the true nature of the Carnian events and does not match evidence archived in geological records for distinct successive geochemical, sedimentological and biological changes. Ruffell and colleagues had already pointed out that the NCIE marking the onset of the CPE "best approximates an 'event' as in event stratigraphy, as opposed to the bulk of the Carnian, which we term the Carnian Humid Episode", concluding that "the two must no longer be confused in the literature" (Ruffell et al., 2016). At the time of the review by Ruffell et al. (2016) the presence of a further 3 NCIEs during the CPE was unknown (Sun et al., 2016; Miller et al., 2017; Dal Corso et al., 2018), and their suggestion was only partially followed in later literature.

Lucas and Hounslow proposed a profound change of the Late Triassic chronostratigraphy, including up-ranking the Carnian Stage and its substages (Lucas, 2013; Hounslow and Lucas, 2023). Among the many considerations, their rationale states that the revision "would greatly assist more precise chronostratigraphic correlation connected with events associated with the CPE, events which are known to cross the Julian-Tuvalian boundary" (Hounslow and Lucas, 2023). I share this view. Their suggestion clearly shows the need to revise the Upper Triassic chronostratigraphy to simplify correlations and age determinations (Hounslow and Lucas, 2023)—the Carnian is one of the longest stages of the Phanerozoic, and the Norian is by far the longest—but formal definition of Stages is done by the Subcommission on Triassic Stratigraphy (https://stratigraphy.org/statutes). In lights of the proposal of Hounslow and Lucas, and of possible future formal outcomes on the topic, I here suggest to revise firstly the substages of the Carnian.

Subdivision of the Carnian into substages was originally made by Mojsisovics and colleagues according to their ammonoid zones, i.e. *Trachyceras aon* (Cordevolian), Trachyceras aonoides (Julian) and *Tropites subbullatus* (Tuvalian) (Mojsisovics et al., 1895; Ogg et al., 2020). The use of Cordevolian has gradually almost disappeared from the literature since the 1970s (e.g., Krystyn, 1978; Gallet et al., 1994; Hornung & Brandner, 2005; Lukeneder & Lukeneder, 2015; Dal Corso et al., 2018), although arguments against its disappearance remained and reconsideration has been urged (Kozur, 2003; Bachmann & Kozur, 2004; Kozur & Bachmann, 2010; Lucas, 2013; Zhang et al., 2020). Currently, the most widely used Carnian Stage subdivision scheme includes the Julian (lower Carnian) and the Tuvalian (upper Carnian) substages, which are further divided into the ammonoid biochronozones Julian 1 (*Trachyceras aonoides* Zone) and Julian 2 (*Austrotrachyceras austriacum* Zone), and Tuvalian 1 (*Tropites dilleri* Zone), Tuvalian 2 (*Tropites subbulatus* Zone) and Tuvalian 3 (*Anatropites spinosus* Zone) sensu Gallet et al. (1994). Notably, the Global Stratotype Section and Point (GSSP) for the base of the Carnian is placed at the base of the *Daxatina canadensis* subzone of the *Trachyceraas aonoides* Zone, with the FAD of the cosmopolitan ammonoid *Daxatina canadensis* (Broglio Loriga et al., 1999; Mietto et al., 2012). *Daxatina canadensis* is the first ammonoid Zone of the Carnian in the Geologic Time Scale (GTS) 2020 (Ogg et al., 2020), following the zonation of Jenks et al. (2015; Figure 2).

Kozur & Bachmann argued against the abandonment of the Cordevolian as the first substage of the Carnian, and advised a return to the original subdivision of Mojsisovics because Cordevolian (*Daxatina canadensis–Trachyceras aon*) and Julian (*Trachyceras aonoides–Austrotrachyceras austriacum*) ammonoid faunas are distinct, with the Cordevolian still containing Ladinian elements (e.g., Kozur, 2003; Bachmann & Kozur, 2004). Urlichs (1994) proposed "to abandon the Julian… and to maintain the Cordevolian consisting of the Aon and the Aonoides Zones" (n.b., *Trachyceras aon* and *Trachyceras aonoides* are subzones of the *Trachyceras aonoides* Zone in other biostratigraphies; see Figure 2). This conclusion came from revision of *Trachyceras* ammonoids found in the San Cassiano Formation in the type localities of the Cordevolian and the Julian in the Dolomites, Italy (Urlichs, 1994; but see also Di Bari & Baracca, 1998). Notably, in the Dolomites NCIE-1 of the CPE is recorded at the transition from the San Cassiano Formation and the overlying Heiligkreuz Formation, i.e., transition from *Trachyceras aonoides* to *Austrotrachyceras austriacum* Zones (e.g., Dal Corso et al., 2012; Pecorari et al., 2023). Also, the term "Cordevolian–Julian boundary (sensu Urlichs, 1974) extinction" is used in the literature of the 1980s, and constituted one of the pillars on which the theory of a global CPE was developed by Simms and Ruffell (Benton, 1986; Simms & Ruffell, 1989; Janofske, 1992).

I here propose that a revised substage-level subdivision of the Carnian, with a "Lower Carnian" (*Daxatina canadensis–Trachyceras aonoides* Zones; Julian 1), a "Middle Carnian" (*Austrotrachyceras austriacum* Zone; Julian 2), and an "Upper Carnian" (*Tropites dilleri–Anatropites spinosus* Zones, Tuvalian 1–3; Figure 2), might be more appropriate: "Julian 1" and "Julian 2" are de facto used in the recent literature as (informal) substages of the Carnian, simply because this significantly helps correlations and discussions on the previously discussed Carnian events. Moreover, a rise of ammonoid extinction rates is recorded from the *Trachyceras aonoides* Zone to the *Austrotrachyceras austriacum* Zone, and a major turnover with the rise of the Tropitidae occurs later, at the boundary between the *Austrotrachyceras austriacum* Zone and *Tropites dilleri* Zone (Figure 2; e.g., Simms & Ruffell, 1989; Balini et al., 2010; Jenks et al., 2015; Dal Corso et al., 2020). Magnetostratigraphy from South China and the Germanic Basin, which needs further confirmation, shows that at the onset of the CPE, i.e., across the boundary between *Trachyceras aonoides* and *Austrotrachyceras austriacum* ammonoid Zones, a transition from a ca. 1.3 Myr "long-reversed-polarity-dominated" interval to a "normal-polarity-dominated" interval is recorded (Zhang et al., 2015, 2020). Subdivision of the Carnian into "Early/Lower", "Middle" and "Late/Upper" Carnian simplifies correlation of CPE events and is justified by the clear biotic changes.

Notably, the CPE has been called in the literature also "Middle Carnian Wet Intermezzo" and "mid-Carnian Event" (Kozur & Bachmann, 2010; Ogg 2015; Ogg et al., 2020): however, during a round table at a workshop on the CPE, no consensus could be reached on "mid-Carnian" because "the major concern being the use of "middle Carnian". In the recent literature the Carnian stage is subdivided in two substages, Lower (or Julian) and Upper (or Tuvalian)…, hence, from a chronostratigraphic point of view "Mid-Carnian Episode (or Event)" would be misleading" (Dal Corso et al., 2018a). Informal "middle Carnian" appears extensively in the literature (e.g., Cousminer & Manspeizer, 1976; Witte & Kent, 1989; Cornet & Olsen, 1990; Kozur & Mock, 1991; Kozur & Mostler, 1994; Simms & Ruffell, 1989; Noyan & Kozur, 2007; Tekin & Göncüoglu, 2007; Moix et al., 2007; Pott et al., 2007; Kozur et al., 2009; Kozur & Bachmann, 2010; Kolar-Jurkovšek & Jurkovšek, 2010; Lucas, 2010, 2020; Franz et al., 2014; Zhang et al., 2015; Ogg 2015; Miller et al., 2017; Forel et al., 2017; Bernardi et al., 2018; Jin et al. 2023). However, in many cases, "middle Carnian" has been used as synonym of Julian as in the three-substage subdivision of the Carnian into Cordevolian, Julian and Tuvalian. Hence, the here proposed substages would partially alter the original subdivision of Mojsisivics and colleagues (1895; Figure 2), and could potentially generate some confusion, especially when referring to older literature. Moreover, my short discussion is focused only on Tethyan ammonoid zonation, and the impact (and correlation) of the revised substages on other biogeographical provinces has not been analyzed. Conodont and sporomorph biozonations, which are very important for correlation of Carnian successions, have also not been considered here. A larger and deeper discussion of Carnian stratigraphy is required to present a more formal proposal for a revision of the Carnian Stage, but this is beyond the scope of this paper, which primarily aims at showing the need to change perspective on the events that marked the Carnian, and how this could benefit from revision of Carnian substages. I here submit my suggestion to the stratigraphers of the Triassic with the aim of fostering further discussions.

Pending validation from the community, the Carnian events could be named, in stratigraphic order from older to youngest, Early–Middle Carnian Event (EMCE; NCIE-1), Middle Carnian Event (MCE; NCIE-2), Middle–Late Carnian Event (MLCE; NCIE-3) and Late Carnian Event (LCE; NCIE-4) (Figure 2). "Carnian Pluvial Episode" should be abandoned, but it remains relevant that these Carnian events occurred close in time—in a maximum timeframe of 2.5 Myr—as observed for similar successive events during other key intervals of the Mesozoic, e.g., in the end Permian – Early Triassic, Late Triassic, and Early Jurassic (Figure 1).

CONCLUSIONS

The large body of data that have been collected in the last decade show multiple global C-isotope excursions during the Carnian, early Late Triassic. Each C-cycle disruption, and inferred consequent climate change, appear to have had a relatively short duration of tens of thousands of years, which is comparable to the duration of the C-isotope excursions that are recorded in coincidence to major Phanerozoic events. However, the interval of the Carnian that encompassed all these discrete events, i.e., the entire so-called Carnian Pluvial Episode (CPE), lasted for up to 2.5 Myrs. Approaching the Carnian C-cycle perturbations as separate events, possibly linked to different triggers and with different impacts on the environment and biota, is necessary to better understand the climatic evolution and extinctions/recovery patterns, and to allow proper comparisons with other Phanerozoic events. A re-evaluation of the substage-level subdivision of the Carnian Stage could help improving stratigraphic correlations of these events.

ACKNOWLEDGMENTS

I am grateful to David B. Kemp (CUG Wuhan, China) and Guido Roghi (IGG-CNR, Italy) for comments on the original draft of this paper. I also thank Piero Gianolla (University of Ferrara, Italy) and Nereo Preto (University of Padova, Italy) for the invaluable many discussions on CPE and Triassic stratigraphy we have had for many years. I thank Mark Hounslow and Piero Gianolla, and the editor Christopher McRoberts for the constructive revisions and precious suggestions that greatly helped improving the manuscript. The National Natural Science Foundation of China is acknowledged for funding (NSFC: 42172031).

REFERENCES

Al-Suwaidi, A.H., Ruhl, M., Jenkyns, H.C., Damborenea, S.E., Manceñido, M.O., Condon, D.J., Angelozzi, G.N., Kamo, S.L., Storm, M., Riccardi, A.C. & Hesselbo, S.P. 2022. New age constraints on the Lower Jurassic Pliensbachian–Toarcian Boundary at Chacay Melehue (Neuquén Basin, Argentina). Scientific Reports, 12: 4975.

Atkinson, J.W. & Wignall, P.B. 2019. How quick was marine recovery after the end-Triassic mass extinction and what role did anoxia play? Palaeogeography, Palaeoclimatology, Palaeoecology, 528: 99–119.

Bachmann, G.H. & Kozur, H.W. 2004. The Germanic Triassic: Correlations with the international chronostratigraphic scale, numerical ages and Milankovitch cyclicity. Hallesches Jahrbuch für Geowissenschaften, B26: 17–62.

Balini, M., Lucas, S.G., Jenks, J.F. & Spielmann, J.A. 2010. Triassic ammonoid biostratigraphy: An overview. Geological Society Special Publications, 334.

Baranyi, V., Jin, X., Dal Corso, J., Li, B. & Kemp, D.B. 2024. Vegetation response to climate change during an Early Jurassic hyperthermal event (Jenkyns Event) from Northern China (Ordos Basin). Palaeogeography, Palaeoclimatology, Palaeoecology, 643: 112180.

Baranyi, V., Miller, C.S., Ruffell, A., Hounslow, M.W. & Kürschner, W.M. 2019. A continental record of the Carnian Pluvial Episode (CPE) from the Mercia mudstone group (UK): Palynology and climatic implications. Journal of the Geological Society London, 176: 149–166.

Benton, M.J. 1986. More than one event in the late Triassic mass extinction. Nature, 321: 857–861.

Bernardi, M., Gianolla, P., Petti, F.M., Mietto, P. & Benton, M.J. 2018. Dinosaur diversification linked with the Carnian Pluvial Episode. Nature, Communications 9: 1499.

Broglio Loriga, C., Cirilli, S., De Zanche, V., Bari, D. D. I., Gianolla, P., Laghi, G. F., Lowrie, W., Manfrin, S., Mastandrea, A., Mietto, P., Muttoni, G., Neri, C., Posenato, R., Rechichi, M., Rettori, R. & Roghi, G. 1999. The Prati di Stuores/Stuores Wiesen section (Dolomites, Italy): A candidate Global Stratotype Section and Point for the base of the Carnian Stage. Rivista Italiana di Paleontologia e Stratigrafia, 105(1): 37–78.

Burgess, S.D., Bowring, S. & Shen, S.Z. 2014. High-precision timeline for Earth's most severe extinction. Proceedings of the National Academy of Sciences of the United States of America, 111: 3316–3321.

Burgess, S.D., Muirhead, J.D. & Bowring, S.A. 2017. Initial pulse of Siberian Traps sills as the trigger of the end-Permian mass extinction. Nature Communications, 8: 164.

Chen, Y., Krystyn, L., Orchard, M.J., Lai, X.L. & Richoz, S. 2016. A review of the evolution, biostratigraphy, provincialism and diversity of Middle and early Late Triassic conodonts. Papers in Palaeontology, 2: 235–263.

Cornet, B. & Olsen, P.E. 1990. Early to Middle Carnian (Triassic) flora and fauna of the Richmond and Taylorsville basins, Virginia and Maryland, U.S.A: Guidebook No. I, Virginia Museum of Natural History, Martinsville, 83 pp.

Cousminer, H. & Manspeizer, W. 1976. Triassic Pollen Date Moroccan High Atlas and the Incipient Rifting of Pangea as Middle Carnian. Science, 191(4230): 943–945.

Dai, X., Davies, J.H.F.L., Yuan, Z., Brayard, A., Ovtcharova, M., Xu, G., Liu, X., Smith, C.P.A., Schweitzer, C.E., Li, M., Perrot, M.G., Jiang, S., Miao, L., Cao, Y., Yan, J., Bai, R., Wang, F., Guo, W., Song, H., Tian, L., Dal Corso, J., Liu, Y., Chu, D. & Song, H. 2023. A Mesozoic fossil lagerstätte from 250.8 million years ago shows a modern-type marine ecosystem. Science, 379(6632): 567–572.

Dal Corso, J., Benton, M.J., Bernardi, M., Franz, M., Gianolla, P., Hohn, S., Kustatscher, E., Merico, A., Roghi, G., Ruffell, A., Ogg, J.G., Preto, N., Schmidt, A.R., Seyfullah, L.J., Simms, M.J., Shi, Z. & Zhang, Y. 2018a. First workshop on the Carnian Pluvial Episode (Late Triassic): a report. Albertiana, 44: 49–57.

Dal Corso, J., Bernardi, M., Sun, Y., Song, H., Seyfullah, L.J., Preto, N., Gianolla, P., Ruffell, A., Kustatscher, E., Roghi, G., Merico, A., Hohn, S., Schmidt, A.R., Marzoli, A., Newton, R.J., Wignall, P.B. & Benton, M.J. 2020. Extinction and dawn of the modern world in the Carnian (Late Triassic). Science Advances, 6(38): eaba0099.

Dal Corso, J., Gianolla, P., Newton, R.J., Franceschi, M., Roghi, G., Caggiati, M., Raucsik, B., Budai, T., Haas, J. & Preto, N. 2015. Carbon isotope records reveal synchronicity between carbon cycle perturbation and the "Carnian Pluvial Event" in the Tethys realm (Late Triassic). Global and Planetary Change, 127: 79–90.

Dal Corso, J., Gianolla, P., Rigo, M., Franceschi, M., Roghi, G., Mietto, P., Manfrin, S., Raucsik, B., Budai, T., Jenkyns, H.C., Reymond, C.E., Caggiati, M., Gattolin, G., Breda, A., Merico, A. & Preto, N. 2018b. Multiple negative carbon-isotope excursions during the Carnian Pluvial Episode (Late Triassic). Earth Science Reviews, 185: 732–750.

Dal Corso, J., Mietto, P., Newton, R.J., Pancost, R.D., Preto, N., Roghi, G. & Wignall, P.B. 2012. Discovery of a major negative $\delta^{13}C$ spike in the Carnian (Late Triassic) linked to the eruption of Wrangellia flood basalts. Geology, 40: 79–82.

Dal Corso, J., Mills, B.J.W., Chu, D., Newton, R.J. & Song, H. 2022. Background Earth system state amplified Carnian (Late Triassic) environmental changes. Earth and Planetary Science Letters, 578: 117321.

Dal Corso, J., Sun, Y. & Kemp, D.B. 2024. Palaeogeographic heterogeneity of large-amplitude changes in marine sedimentation rates during the Carnian Pluvial Episode (Late Triassic). Global and Planetary Change, 237: 104437.

Davies, J.H.F.L., Marzoli, A., Bertrand, H., Youbi, N., Ernesto, M. & Schaltegger, U. 2017. End-Triassic mass extinction started by intrusive CAMP activity. Nature Communications, 8: 15596.

Di Bari, D. & Baracca, A. 1998. Late Triassic (Carnian) Foraminifers of Northeastern Cortina d'Ampezzo (Tamarin, San Cassiano Fm., Dolomites, Italy). Annali del Museo Civico di Rovereto, 12: 117–146.

Dickens, G.R., O'Neil, J.R., Rea, D.K. & Owen, R.M. 1995. Dissociation of oceanic methane hydrate as a cause of the carbon isotope excursion at the end of the Paleocene. Paleoceanography, 10: 965–971.

Forel, M.-B., Tekin, U.K., Okuyucu, C., Bedi, Y., Tuncer, A. & Crosquin, S. 2017. Discovery of a long-term refuge for ostracods (Crustacea) after the end-Permian extinction: a unique Carnian (Late Triassic) fauna from the Mersin Mélange, southern Turkey. Journal of Systematic Palaeontology, 17(1): 9–58.

Franz, M., Nowak, M., Berner, U., Heunisch, C., Bandel, K., Rohling H.-G. & Wolfgramm, M. 2014. Eustatic control on epicontinental basins: The example of the Stuttgart Formation in the Central European Basin (Middle Keuper, Late Triassic). Global and Planetary Change, 122: 305–329.

Fu, X., Wang, J., Wen, H., Wang, Z., Zeng, S., Song, C., Chen, W. & Wan, Y. 2020. A possible link between the Carnian Pluvial Event, global carbon-cycle perturbation, and volcanism: New data from the Qinghai-Tibet Plateau. Global and Planetary Change, 194: 103300.

Furin, S., Preto, N., Rigo, M., Roghi, G., Gianolla, P., Crowley, J.L. & Bowring, S.A. 2006. High-precision U-Pb zircon age from the Triassic of Italy: Implications for the Triassic time scale and the Carnian origin of calcareous nannoplankton and dinosaurs. Geology, 34: 1009–1012.

Gallet, Y., Besse, J., Krystyn, L., Théveniaut, H. & Marcoux, J. 1994. Magnetostratigraphy of the Mayerling section (Austria) and Erenkolu Mezarlik (Turkey) section: Improvement of the Carnian (Late Triassic) magnetic polarity time scale. Earth and Planetary Science Letters, 125(1–4): 173–191.

Gattolin, G., Preto, N., Breda, A., Franceschi, M., Isotton, M. & Gianolla, P. 2015. Sequence stratigraphy after the demise of a high-relief carbonate platform (Carnian of the Dolomites): Sea-level and climate disentangled. Palaeogeography, Palaeoclimatology, Palaeoecology, 423: 1–17.

Greene, A.R., Scoates, J.S., Weis, D., Katvala, E.C., Israel, S. & Nixon, G.T. 2010. The architecture of oceanic plateaus revealed by the volcanic stratigraphy of the accreted Wrangellia oceanic plateau. Geosphere, 6: 47–73.

Heimdal, T.H., Jones, M.T. & Henrik, H.S. 2020. Thermogenic carbon release from the Central Atlantic magmatic province caused major end-Triassic carbon cycle perturbations. Proceedings of the National Academy of Sciences of the United States of America, 117(22): 11968–11974.

Hornung, T. & Brandner, R. 2005. Biochronostratigraphy of the Reingraben Turnover (Hallstatt Facies Belt): Local black shale events controlled by regional tectonics, climatic change and plate tectonics. Facies, 51: 460–479.

Hornung, T., Brandner, R., Krystyn, L., Joachimski, M. M. & Keim, L. 2007a. Multistratigraphic constraints on the NW Tethyan "Carnian crisis." New Mexico Museum of Natural History and Science Bulletin, 41: 59–67.

Hornung, T., Krystyn, L. & Brandner R. 2007b. A Tethys-wide mid-Carnian (Upper Triassic) carbonate productivity crisis: Evidence for the Alpine Reingraben Event from Spiti (Indian Himalaya)? Journal of Asian Earth Sciences, 30: 285–302.

Hounslow, M. W. & Gallois, R. 2023. Magnetostratigraphy of the Mercia Mudstone Group (Devon, UK): implications for regional relationships and chronostratigraphy in the Middle to Late Triassic of Western Europe. Journal of the Geological Society London, 180(4): jgs2022-173.

Hounslow, M.W., Harris, S.E., Karloukovski, V. & Mørk, A. 2022. Geomagnetic polarity and carbon isotopic stratigraphic assessment of the late Carnian -earliest Norian in Svalbard: evidence for a major hiatus and improved Boreal to Tethyan correlation. Norwegian Journal of Geology, 102: 202204.

Hounslow, M.W. & Lucas, S.G. 2023. A proposal for new chronostratigraphic stage subdivisions of the Upper Triassic series. Albertiana, 48: 1–10.

Hu, X.-M., Jiang, J.-X., Cai, Y., Han, Z. & Xu, Y.-W. 2024. Temporal scaling of carbon emission accumulations and rates of the Meso-Cenozoic hyperthermal events: implication to the Anthropocene global warming. Mesozoic, 1: 396–407.

Janofske, D. 1992. Kalkiges Nannoplankton, insbesondere kalkige Dinoflagellaten-Zysten der alpinen Ober-Trias: Taxonomie, Bio-stratigraphie und Bedeutung für die Phylogenie der Peridiniales. Berliner Geowissenschaftliche Abhandlungen, 4: 1–53.

Jenks, J. F., Monnet, C., Balini, M., Brayard, A. & Meier, M. 2015. Biostratigraphy of Triassic Ammonoids. In, Klug, C., Korn, D., De Baets, K., Kruta, I. & Mapes, R.H. (eds.), Ammonoid Paleobiology: From macroevolution to paleogeography. Springer Dordrecht, pp. 329–388.

Jin, X., Franceschi, M., Martini, R., Shi, Z., Gianolla, P., Rigo, M., Wall, C.J., Schmitz, M.D., Lu, G., Du, Y., Huang, X. & Preto, N. 2022. Eustatic sea-level fall and global fluctuations in carbonate production during the Carnian Pluvial Episode. Earth and Planetary Science Letters, 594: 117698.

Jin, X., Gianolla, P., Shi, Z., Franceschi, M., Caggiati, M., Du, Y. & Preto, N. 2020. Synchronized changes in shallow water carbonate production during the Carnian Pluvial Episode (Late Triassic) throughout Tethys. Global and Planetary Change, 184: 103035.

Jin, X., Tomimatsu, Y., Yin, R., Onoue, T., Franceschi, M., Grasby, S.E., Du, Y. & Rigo, M. 2023. Climax in Wrangellia LIP activity coincident with major Middle Carnian (Late Triassic) climate and biotic changes: Mercury isotope evidence from the Panthalassa pelagic domain. Earth and Planetary Science Letters, 607: 118075.

Kemp, D.B., Han, Z., Hu, X., Chen, W., Jin, S., Izumi, K., Yan, Q., Baranyi, V., Dal Corso, J. & Ge, Y. 2024a. Global hydroclimate perturbations during the Toarcian oceanic anoxic event. Earth Science Reviews, 258: 104946.

Kemp, D.B., Ramezani, J., Izumi, K., Al-Suwaidi, A., Huang, C., Chen, W. & Zhu, Y. 2024b. The timing and duration of large-scale carbon release in the Early Jurassic. Geology, 52(12): 891–895.

Kolar-Jurkovšek, T. & Jurkovšek, B. 2010. New paleontological evidence of the Carnian strata in the Mežica area (Karavanke Mts, Slovenia): Conodont data for the Carnian Pluvial Event. Palaeogeography, Palaeoclimatology, Palaeoecology, 290(1–4): 81–88.

Kozur, H.W. 2003. Integrated ammonoid, conodont and radiolarian zonation of the Triassic and some remarks to Stage/Substage subdivision and the numeric age of the Triassic stages. Albertiana, 28: 57–83.

Kozur, H.W. & Mock, R. 1991. New Middle Carnian and Rhaetian Conodonts from Hungary and the Alps. Stratigraphic Importance and Tectonic Implications for the Buda Mountains and Adjacent Areas. Jahrbuch der Geologischen Bundesanstalt, 134(2): 271–297.

Kozur, H.W. & Mostler, H. 1994. Anisian to Middle Carnian radiolarian zonation and description of some stratigraphically important radiolarians. Geologisch-Paläontologische Mitteilungen Innsbruck, Sonderband 3: 39–255.

Kozur, H.W. & Bachmann, G.H. 2010. The Middle Carnian Wet Intermezzo of the Stuttgart Formation (Schilfsandstein), Germanic Basin. Palaeogeography, Palaeoclimatology, Palaeoecology, 290: 107–119.

Kozur, H.W., Moix, P. & Ozsvart, P. 2009. New Spumellaria (Radiolaria) from the Early Tuvalian Spongotortilispinus moixi Zone of Southeastern Turkey, with some Remarks on the Age of this Fauna. Jahrbuch der Geologischen Bundesanstalt, 149:25–59.

Krystyn, L. 1978. Eine neue Zonengliederung im Alpin-Mediterranen Unterkarn. Schr. Erdwissenschaftlichen Kommission, Österreichische Akademie der Wissenschaften, 4: 37–55.

Lassiter, J. C., Depaolo, D. J. & Mahoney, J. J. 1995. Geochemistry of the wrangellia flood basalt province: Implications for the role of continental and oceanic lithosphere in flood basalt genesis. Journal of Petrology, 36: 983–1009.

Lestari, W., Al-Suwaidi, A., Fox, C. P., Vajda, V. & Hennhoefer, D. 2024. Carbon cycle perturbations and environmental change of the Middle Permian and Late Triassic Paleo-Antarctic circle. Scientific Reports, 14: 9742.

Li, M., Bralower, T. J., Kump, L. R., Self-Trail, J. M., Zachos, J. C., Rush, W. D. & Robinson, M.M. 2022. Astrochronology of the Paleocene-Eocene Thermal Maximum on the Atlantic Coastal Plain. Nature Communications, 13: 5618.

Lowery, C. M., Bralower, T. J., Owens, J. D., Rodríguez-Tovar, F. J., Jones, H., Smit, J., Whalen, M.T., Claeys, P., Farley, K., Gulick, S.P.S., Morgan, J.V., Green, S., Chenot, E., Christeson, G.L., Cockell, C.C., Coolen, M.J.L., Ferriere, L., Gebhardt, C., Goto, K., Kring, D.A., Lofi, J., Ocampo-Torres, R., Perez-Cruz, L., Pickersgill, A.E., Poelchau, M.H., Rae, A.S.P., Rasmussen, C., Rebolledo-Vieyra, M., Riller, U., Sato, H., Tikoo, S.M., Tomioka, N., Urrutia-Fucugauchi, J., Vellekoop, J., Wittmann, A., Xiao, L., Yamaguchi, K.E. & Zylberman, W. 2018. Rapid recovery of life at ground zero of the end-Cretaceous mass extinction. Nature, 558: 288–291.

Lu, J., Zhang, P., Dal Corso, J., Yang, M., Wignall, P. B., Greene, S. E., Shao, L., Lyu, D. & Hilton J. 2021. Volcanically driven lacustrine ecosystem changes during the Carnian Pluvial Episode (Late Triassic). Proceedings of the National Academy of Sciences, 118: e2109895118.

Lucas, S.G. 2010. The Triassic timescale: an introduction. Geological Society, London, Special Publications, 334: 1–16.

Lucas, S.G. 2013. A new Triassic timescale. In, Tanner, L.H., Spielmann, J.A. & Lucas, S.G. (eds.), The Triassic System. New Mexico Museum of Natural History and Science Bulletin, pp. 366–374.

Lucas, S.G. 2020. Biochronology of Late Triassic Metoposauridae (Amphibia, Temnospondyli) and the Carnian Pluvial Episode. Annales Societatis Geologorum Poloniae, 90: 409–418.

Lukeneder, S. & Lukeneder, A. 2015. A new ammonoid fauna from the Carnian (Upper Triassic) Kasimlar Formation of the Taurus Mountains (Anatolia, Turkey). Palaeontology, 57(2): 357–396.

Maron, M., Muttoni, G., Mietto, P. & Gianolla, P. 2024. Magnetostratigraphy of the Punta Grohmann section (Dolomites, Italy): improving the chronology of the Ladinian/Carnian boundary. Palaeogeography, Palaeoclimatology, Palaeoecology, 639: 112077.

Martinez, M., Krencker, F.N., Mattioli, E. & Bodin, S. 2017. Orbital chronology of the Pliensbachian – Toarcian transition from the Central High Atlas Basin (Morocco). Newsletters in Stratigraphy, 50: 47–69.

Mazaheri-Johari, M., Gianolla, P., Mather, T.A., Frieling, J., Chu, D. & Dal Corso, J. 2021. Mercury deposition in Western Tethys during the Carnian Pluvial Episode (Late Triassic). Scientific Reports, 11: 17339.

Mietto, P., Manfrin, S., Preto, N., Rigo, M., Roghi, G., Furin, S., Gianolla, P., Posenato, R., Muttoni, G., Nicora, A., Buratti, N., Cirilli, S., Spötl, C., Ramezani, J. & Bowring, S.A. 2012. The Global boundary Stratotype Section and Point (GSSP) of the Carnian Stage (Late Triassic) at Prati di Stuores/Stuores Wiesen Section (Southern Alps, NE Italy). Episodes, 35: 414–430.

Miller, C.S., Peterse, F., Da Silva, A.C., Baranyi, V., Reichart, G.J. & Kürschner, W.M. 2017. Astronomical age constraints and extinction mechanisms of the Late Triassic Carnian crisis. Scientific Reports, 7: 2557.

Mojsisovics, E. von, Waagen, W.H. & Diener, C. 1895. Entwurf einer Gliederung der pelagischen Sedimente des Trias-Systems. Sitzungberichte der Akademie der Wissenschaften in Wien, 104: 1271–1302.

Moix, P., Kozur, H., Stampfli, G.M. & Mostler, H. 2007. New paleontological, biostratigraphic and paleogeographic results from the Triassic of the Mersin Melange, SE Turkey. In, Lucas, S.G. & Spielmann, J.A. (Eds.): The Global Triassic. Bulletin of the New Mexico Museum of Natural History and Science, 41: 282-305.

Mueller, S., Hounslow, M.W. & Kürschner, W. M. 2016a. Integrated stratigraphy and palaeoclimate history of the Carnian Pluvial event in the Boreal realm; new data from the upper Triassic Kapp Toscana group in central Spitsbergen (Norway). Journal of the Geological Society London, 173: 186–202.

Mueller, S., Krystyn, L. & Kürschner, W. M. 2016b. Climate variability during the Carnian Pluvial Phase - A quantitative palynological study of the Carnian sedimentary succession at Lunz am See, Northern Calcareous Alps, Austria. Palaeogeography, Palaeoclimatology, Palaeoecology, 441: 198–211.

Noyan, O. & Kozur, H.W. 2007. Revision of the late Carnian early Norian conodonts from the Stefanion section (Argolis, Greece) and their palaeobiogeographic implications. Neues Jahrbuch für Geologie und Paläontologie – Abhandlungen, 245(2): 159–178.

Ogg, J.G. 2015. The mysterious Mid-Carnian "Wet Intermezzo" global event. Journal of Earth Science, 26: 181–191.

Ogg, J.G., Chen, Z.Q., Orchard, M.J. & Jiang, H. S. 2020. The Triassic Period. In, Gradstein, F.M., Ogg, J.G., Schitz, M.D., Ogg, G.M. (eds.), Geologic Time Scale 2020. Elsevier, pp. 903–953.

Pecorari, M., Caggiati, M., Dal Corso, J., Cruciani, G., Tateo, F., Chu, D. & Gianolla, P. 2023. Weathering and sea level control on siliciclastic deposition during the Carnian Pluvial Episode (Southern Alps, Italy). Palaeogeography, Palaeoclimatology, Palaeoecology, 617: 111495.

Pott, C., Krings, M. & Kerp, H. 2007. First record of *Nilssoniopteris* (Gymnospermophyta, Bennettitales) from the Carnian (Upper Triassic) of Lunz, lower Austria. Palaeontology, 50(5): 1299–1318.

Rahman, N.U., Xian, B., Fang, L., Chen, S., Chen, P., Ullah, Z. & Wang, P. 2024. Volcanically Driven Terrestrial Environmental Perturbations during the Carnian Pluvial Episode in the Eastern Tethys. Acta Geologica Sinica (English Edition), 98: 753–770.

Rigo, M., Mazza, M., Karádi, V. & Nicora, A. 2018. New Upper Triassic Conodont Biozonation of the Tethyan Realm. In, Tanner, L. (ed.), The Late Triassic World. Springer Cham, pp. 189–235.

Rigo, M., Preto, N., Roghi, G., Tateo, F. & Mietto, P. 2007. A rise in the Carbonate Compensation Depth of western Tethys in the Carnian (Late Triassic): Deep-water evidence for the Carnian Pluvial Event. Palaeogeography, Palaeoclimatology, Palaeoecology, 246: 188–205.

Roghi, G., Gianolla, P., Minarelli, L., Pilati, C. & Preto, N. 2010. Palynological correlation of Carnian humid pulses throughout western Tethys. Palaeogeography, Palaeoclimatology, Palaeoecology, 290: 89–106.

Ruffell, A., Simms, M.J. & Wignall, P.B. 2016. The Carnian Humid Episode of the Late Triassic: A review. Geological Magazine, 153: 271–284.

Ruhl, M., Deenen, M.H.L., Abels, H.A., Bonis, N.R., Krijgsman, W. & Kürschner, W.M. 2010. Astronomical constraints on the duration of the early Jurassic Hettangian stage and recovery rates following the end-Triassic mass extinction (St Audrie's Bay/East Quantoxhead, UK). Earth and Planetary Science Letters, 295: 262–276.

Schlager, W. & Schöllnberger, W., 1974. Das Prinzip stratigraphischer Wenden in der Schichtfolge der Nördlichen Kalkalpen. Mitteilungen der Österreichischen Geologischen Gesellschaft, 66–67: 165–193.

Shi, Z., Jin, X., Preto, N., Rigo, M., Du, Y. & Han, L. 2019. The Carnian Pluvial Episode at Ma'antang, Jiangyou in upper Yangtze block, Southwestern China. Journal of the Geological Society London, 176: 197–207.

Simms, M.J. & Ruffell, A.H. 1989. Synchroneity of climatic change and extinctions in the Late Triassic. Geology, 17: 265–268.

Simms, M.J. & Ruffell, A.H. 2018. The Carnian Pluvial Episode: From discovery, through obscurity, to acceptance. Journal of the Geological Society London, 175: 989–992.

Sun, Y.D., Richoz, S., Krystyn, L., Zhang, Z.T. & Joachimski, M.M. 2019. Perturbations in the carbon cycle during the Carnian Humid Episode: Carbonate carbon isotope records from southwestern China and Northern Oman. Journal of the Geological Society London, 176: 167–177.

Sun, Y.D., Wignall, P.B., Joachimski, M.M., Bond, D.P.G., Grasby, S.E., Lai, X.L., Wang, L.N., Zhang, Z.T. & Sun, S. 2016. Climate warming, euxinia and carbon isotope perturbations during the Carnian (Triassic) Crisis in South China. Earth and Planetary Science Letters, 444: 88–100.

Svensen, H.H., Frolov, S., Akhmanov, G.G., Polozov, A.G., Jerram, D.A., Shiganova, O.V., Melnikov, N.V., Iyer, K & Planke, S. 2018. Sills and gas generation in the Siberian Traps. Philosophical Transactions of the Royal Society A: Mathematical, Physical and Engineering Sciences, 376: 20170080.

Tekin, U.K. & Göncüoğlu, M.C. 2007. Discovery of the oldest (Upper Ladinian to Middle Carnian) radiolarian assemblages from the Bornova Flysch Zone in western Turkey: Implications for the evolution of the Neotethyan Izmir-Ankara ocean. Ofioliti, 32(2):131–150.

Tomimatsu, Y., Nozaki, T., Sato, H., Takaya, Y., Kimura, J.I., Chang, Q., Naraoka, H., Rigo, M. & Onoue, T. 2021. Marine osmium isotope record during the Carnian "pluvial episode" (Late Triassic) in the pelagic Panthalassa Ocean. Global and Planetary Change, 197: 103387.

Tóth, E., Baranyi, V., Karádi, V., Jin, X. & Budai, T. 2024. Ostracod turnover during the Carnian Pluvial Episode (Late Triassic) in the Western Neotethys. Palaeogeography, Palaeoclimatology, Palaeoecology, 650: 112379.

Urlichs, M. 1974. Zur Stratigraphie und Ammonitenfauna der Cassianer Schichten von Cassian (Dolomiten/Italien). In, Zapfe, H. (ed.), Die Stratigraphie der alpin-mediterranen Trias. Schriftenreihe der Erdwissenschaftlichen Kommission der Österreichischen: Akademie der Wissenschaften, pp. 207–222.

Urlichs, M. 1994. *Trachyceras* Laube 1869 (Ammonoidea) from the Lower Carnian (Upper Triassic) of the Dolomites. Stuttgarter Beiträge zur Naturkunde Serie B (Geologie und Paläontologie), 217: 1–55.

Witte, W.K. & Kent, D.K. 1989. A middle Carnian to early Norian (~225 Ma) paleopole from sediments of the Newark Basin, Pennsylvania. Geological Society of America Bulletin, 101(9): 1118–1126.

Yager, J.A., West, A.J., Corsetti, F.A., Berelson, W.M., Rollins, N.E., Rosas, S. & Bottjer, D.J. 2017. Duration of and decoupling between carbon isotope excursions during the end-Triassic mass extinction and Central Atlantic Magmatic Province emplacement. Earth and Planetary Science Letters, 473: 227–236.

Zhang, Q., Fu, X., Wang, J., Mansour, A., Wei, H., Zhang, T. & Wang, M. 2024. Orbitally-paced climate change during the Carnian Pluvial Episode. Earth and Planetary Science Letters, 626: 118546.

Zhang, Y., Li, M., Ogg, J.G., Montgomery, P., Huang, C., Chen, Z.Q., Shi, Z., Enos, P. & Lehrmann, D.J. 2015. Cycle-calibrated magnetostratigraphy of middle Carnian from South China: Implications for Late Triassic time scale and termination of the Yangtze Platform. Palaeogeography, Palaeoclimatology, Palaeoecology, 436: 135–166.

Zhang, Y., Ogg, J.G., Franz, M., Bachmann, G.H., Szurlies, M., Röhling, H.G., Li, M., Rolf, C. & Obst, K. 2020. Carnian (Late Triassic) magnetostratigraphy from the Germanic Basin allowing global correlation of the Mid-Carnian Episode. Earth and Planetary Science Letters, 541: 116275.